NANO LETTERS

LETTER

pubs.acs.org/NanoLett

Bovine Serum Albumin−Poly(methyl methacrylate) Nanoparticles: An Example of Frustrated Phase Separation

Jun Ge, Jiandu Lei, and Richard N. Zare*

Department of Chemistry, Stanford University, Stanford, California 94305-5080, United States

ABSTRACT: A new protein−polymer conjugate made of denatured bovine serum albumin (BSA) covalently bonded to poly(methyl methacrylate) (PMMA) is synthesized by attaching PMMA to acryloylated BSA followed by nanoparticle precipitation. Depending on the BSA to PMMA ratio, these conjugates self-assemble into uniform spherical nanoparticles which show "island" growth on the surface of the nanoparticles. This growth is promoted or retarded by exposing the nanoparticles to different solvents, causing the two components to undergo incipient phase separation. Incipient phase separation of the BSA-PMMA conjugate two-component system was observed in single nanoparticles, resulting in "island" growth on the surface of the nanoparticles. Incipient phase separation of the BSA−PMMA conjugate two-component system was observed in single nanoparticles, resulting in "island" growth on the surface of the nanoparticles.

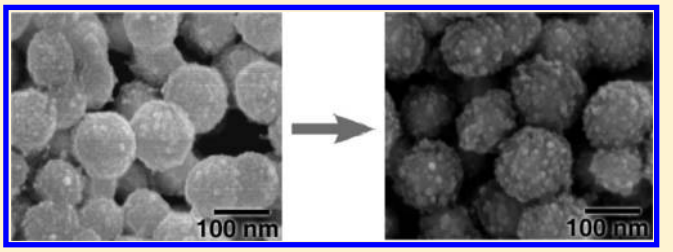

KEYWORDS: Protein−polymer conjugate, nanoparticles, phase separation

The large surface-to-volume ratio of nanoparticles provides one important reason why nanoparticles have many advantages over the same material in bulk. For example, surface properties can regulate stability, solubility, and functionality, which play an important role in many applications.[1−4] In the present study, we have synthesized a new protein−polymer conjugate made of denatured bovine serum albumin (BSA), which is a nutrient to cells, and poly(methyl methacrylate) (PMMA), which is a synthetic thermoplastic polymer. Under certain composition conditions, the resulting BSA−PMMA nanoparticles may be highly spherical in shape and can display incipient phase separation of the two immiscible components, which cause "islands" to appear on the surfaces of the nanoparticles.

Protein−polymer conjugates, which consist of proteins and polymers covalently linked together, have been previously demonstrated to have significant applications in the area of therapeutic protein delivery[5] and biocatalysis.[6−8] Protein−polymer conjugates could be synthesized either by attaching a synthetic polymer to protein[9] or by growing synthetic polymer chains from protein.[7] In this study, PMMA chains were directly grown from acryloylated protein by radical polymerization to form the branched copolymer (Scheme 1).

Each BSA was confirmed to be modified with 51 acryloyl groups as determined by MALDI-TOF mass spectrometry. The content of BSA in the conjugate was varied to be 4, 69, or 82 wt % as determined by ^{1}H NMR. The conjugate in acetonitrile (2.5 mg/mL) was injected into a phosphate buffered saline (pH 7.4) solution to precipitate nanoparticles. As the content of BSA increased from 4, to 69, to 82 wt %, the average size of the nanoparticles increased from 30 to 60 to 90 nm (Figure 1), as determined by scanning electron microscopy (SEM). Dynamic light scattering (DLS) revealed a different set of measurements; the average size decreased from 477 to 336 to 321 nm (also a peak with particle size around 100 nm was shown indicating well-separated nanoparticles presented in this sample). The DLS measurements suggest that in aqueous solution aggregates are formed with low content of BSA while with 82 wt % of BSA in the conjugate the nanoparticles are very well dispersed and readily more separate from each other. The hydrophilic property of BSA and the decrease in the values of the zeta potential of the nanoparticles from −39.4 to −45.7 to −51.6 mV might be considered to be two main factors that contribute to the more stable dispersion of nanoparticles with increasing content of BSA in the conjugates.

Scheme 1. Synthesis of Denatured BSA−PMMA Conjugate[a]

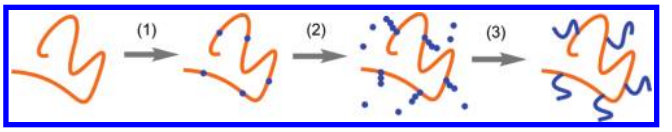

[a] Key: (1) acryloyl groups are chemically introduced to denatured BSA in DMSO; (2) radical polymerization of MMA with BSA is induced by addition of AIBN; (3) the protein−polymer conjugate is precipitated by adding the antisolvent that is a (1:8 v/v) mixture of methanol and ethyl ether.

More interesting is the morphology of the nanoparticles, which also changed with conjugate composition. At 4 wt % of BSA, irregularly shaped nanoparticles with some agglomeration are formed (Figure 1a). At 69 wt % of BSA, very uniform spherical nanoparticles with smooth surface are formed (Figure 1b). At 82 wt % of BSA, small "islands" were observed to form on the surface of the uniform nanospheres (Figure 1c). Because we

Received: April 18, 2011
Published: May 09, 2011

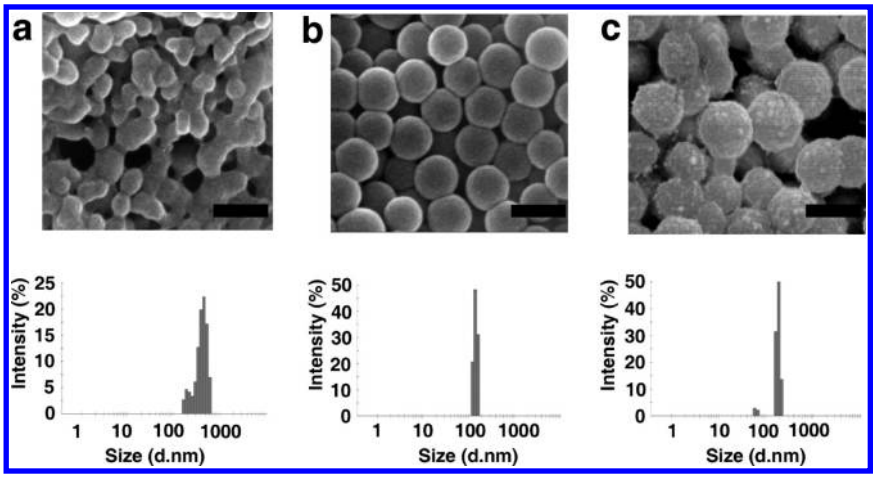

Figure 1. SEM images of BSA−PMMA nanoparticles made with (a) 4 wt % BSA, (b) 69 wt % BSA, and (c) 82 wt % BSA. Scale bars are 100 nm. The corresponding particle size distribution, determined by dynamic light scattering, is shown below each image.

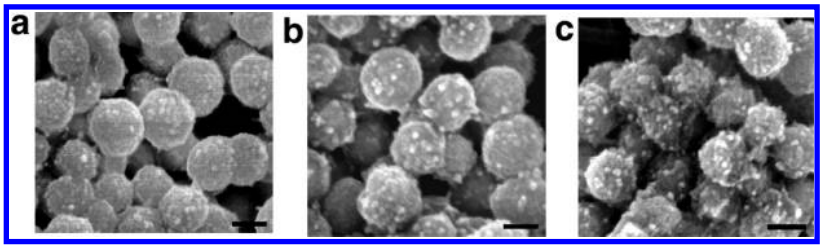

Figure 2. SEM images showing time dependence of the structural change of the BSA82−PMMA18 nanoparticles: (a) day 1; (b) day 7; (c) day 14. Scale bars are 100 nm.

concentrate on the last case, we introduce in what follows the symbol BSA82−PMMA18 for nanoparticles formed with 82% BSA and 18% PMMA.

We have concentrated our attention to the surface morphology of the BSA−PMMA nanospheres having high BSA content. We found from SEM that the amount of "islands" on the surface of the BSA−PMMA nanoparticles gradually increased over a period of 2 weeks when the nanoparticles were incubated in aqueous PBS solution (pH 7.4) without any treatment (Figure 2). During this time, the hydrodynamic size and the zeta potential of the nanoparticles remained unchanged, indicating no obvious degradation of the nanoparticles, a conclusion that is also consistent with the SEM observations.

To gain more information about the surface morphology, we chemically attached FITC to the BSA component of the conjugate, followed by the same nanoprecipitation procedure to make the BSA82−PMMA18 nanoparticles in aqueous PBS (pH 7.4). The fluorescent spectrum was recorded (Figure 3) during the incubation period of 2 weeks. The maximum emission wavelength shifts from 538 nm (day 1) to 526 nm (day 14). Along with the blue shift, the fluorescent intensity was also observed to increase. Self-quenching of FITC dye is one of the oldest observations in fluorescence spectroscopy[10] and is caused by resonance energy transfer (RET) between FITC molecules. In the case of FITC the Forster distance for RET is about 42 Å.[11] Thus, from the fluorescence spectroscopy result, we propose that at the beginning of the incubation, the BSA component with FITC attached to it was confined in a relatively small region where self-quenching of FITC molecules occurred, resulting in a decrease of fluorescent

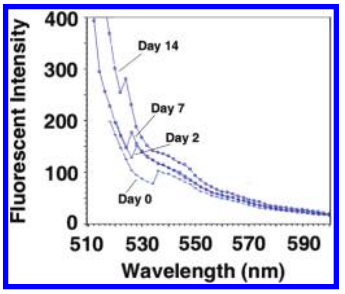

Figure 3. The change of fluorescent spectrum of FITC attached to BSA component in the BSA82−PPMA18 nanoparticles during incubation in PBS at pH 7.4.

intensity. During the incubation period, the BSA component gradually transferred from the inside region to the outer region of the nanoparticles, which resulted in a more separated FITC molecules and thus a decrease of self-quenching.

Let us consider the Flory−Huggins theory of mixing[12] as applied to this system. We denote by ϕ the volume fraction of BSA chains, N the number of lattice sites occupied by each molecule (N_{BSA} for the BSA chains; N_{PMMA} for the PMMA chains), and χ the Flory interaction parameter. Then the free energy of mixing is given by

$$\Delta G_{mix} = kT\left[\frac{\varphi}{N_{BSA}}\ln\varphi + \frac{1-\varphi}{N_{PMMA}}\ln(1-\varphi) + \chi\varphi(1-\varphi)\right] \quad (1)$$

dx.doi.org/10.1021/nl201303q |*Nano Lett.* 2011, 11, 2551–2554

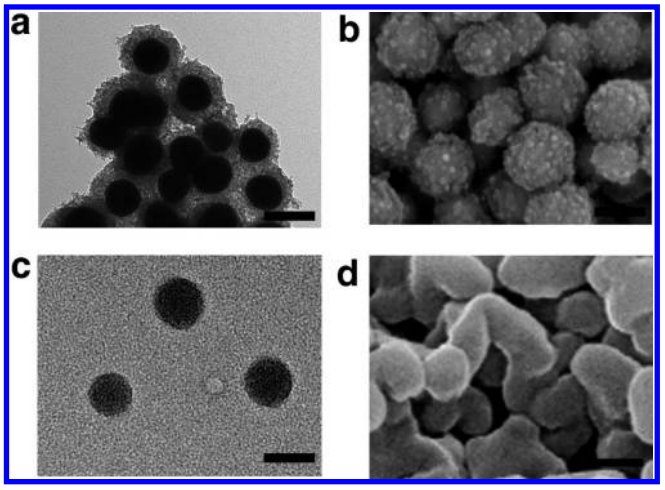

Figure 4. Nanoparticle images: (a) TEM of BSA82−PMMA18 nanoparticles incubated in aqueous PBS solution for 14 days; (b) SEM of the same BSA82−PMMA18 nanoparticles; (c) TEM of BSA82−PMMA18 nanoparticles in acetonitrile for 14 days; (d) SEM of the same BSA82−PMMA18 nanoparticles. Scale bars are 100 nm.

The second derivative of the free energy gives the spinodal and consequently the critical interaction parameter for phase separation, which is expressed as

$$\chi_c = \frac{v_0}{2}\left(\frac{1}{\sqrt{v_{BSA}}} + \frac{1}{\sqrt{v_{PMMA}}}\right)^2 \quad (2)$$

where v_0 is the lattice site volume and v_i is the molecular volume of polymer chain i. Knowing the dimension of a single BSA molecule[13] (v_{BSA} = 135cm^3·mol^{-1}) and a MMA monomer[14] (v_{MMA} = 78cm^3·mol^{-1}), and assuming the lattice site volume v_0 equals the volume of MMA monomer, for the BSA82−PMMA18 conjugate (with a molar ratio of repeating units of PMMA to BSA of 144:1 as determined by ^{1}H NMR), we calculate that v_{PMMA} = 11232cm^3·mol^{-1} and the critical interaction parameter χ_c is 0.36. Solubility parameters of PMMA[15] (δ_{PMMA} = 19.0 MPa$^{1/2}$) and BSA[16] (δ_{BSA} = 35.3 MPa$^{1/2}$) yield

$$\chi_{PMMA-BSA} = (\delta_{PMMA} - \delta_{BSA})^2 \frac{v_0}{RT} = 8.75 > \chi_c \quad (3)$$

Hence, Flory−Huggins theory predicts that phase separation is expected to occur in the BSA−PMMA two-component system. At the same time, the connectivity of the copolymers prevents a macroscopic phase separation. As a result of these competing trends in a given solvent, the BSA−PMMA copolymer system self-organizes into complex structures in a single nanoparticle, which is a consequence of what we call frustrated phase separation.

To further understand the self-organization process, we observed the BSA82−PMMA18 nanoparticles after incubation of 14 days in aqueous PBS solution by transmission electron microscopy (TEM), as shown in Figure 4a. This image indicates that an incipient phase separation is occurring in the nanoparticles. A clear delineation of core−shell structure from the periphery of the nanoparticles is caused by the large difference in scattering between BSA and PMMA parts. While most of the PMMA chains are located at the cores of the nanoparticles, in the shells of the nanoparticles BSA chains and PMMA chains interweave together in a complex pattern. This behavior seems

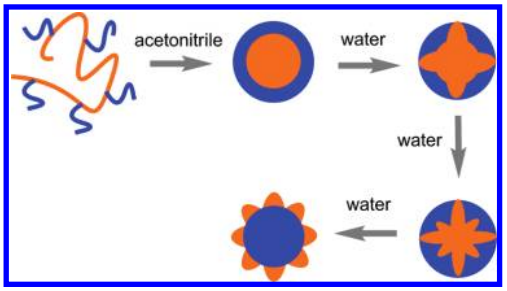

Figure 5. A mechanism for the formation and structural changes of nanoparticles made from BSA−PMMA conjugates. The blue part represents PMMA chains, the yellow part represents BSA component.

to be consistent with the complex surface morphology observed by SEM as shown in Figure 4b.

In sharp contrast, the behavior of the BSA82−PMMA18 nanoparticles in acetonitrile (Figure 4c,d) is markedly different. Unlike the nanoparticles incubated in aqueous solution which are shown in paanels a and b of Figures 4, we cannot discriminate between the BSA and PMMA parts in the nanoparticles in acetonitrile both immediately after dissolving the conjugate in acetonitrile and after incubating it in acetonitrile for 14 days. We conclude that the distribution of two components is relatively uniform and no obvious structure change occurred in acetonitrile.

Figure 5 illustrates a proposed mechanism for frustrated phase separation. Acetonitrile is known to be a good solvent for PMMA but a poor solvent for BSA. Therefore, we suggest that BSA−PPMA nanoparticles formed in acetonitrile have the PMMA located primarily in the shell region of the nanoparticles (Figure 4c,d). Upon the injection of the acetonitrile solution containing the nanoparticles into aqueous solution, PMMA moves to the shell region of the nanoparticles, causing the nanoparticles to precipitate in the aqueous phase with relatively even initial distribution of the PMMA and BSA components (Figure 2a). During the incubation of the nanoparticles in aqueous solution, the BSA part, which is more hydrophilic than the PMMA part, gradually transfers to the outer layer of the nanoparticles and frustrated phase separation between PMMA and BSA parts occurs to form islands on the surface of the nanoparticle. On the other hand, when the BSA82−PMMA18 nanoparticles are soaked in acetonitrile, no change is evident, suggesting that the minority PMMA is unable to cause the majority BSA to appreciably reassemble.

The mechanism accounts for the structural changes observed by SEM, as shown in Figure 2. It also explains the fluorescence experiments shown in Figure 3, which indicates that the BSA gradually migrates from the hydrophobic confined environment to the outer-layer hydrophilic environment.

In conclusion, we synthesized the denatured BSA−PMMA conjugate, from which uniform spherical nanoparticles were prepared by a simple self-assembling process. The nanoparticles exhibit unique phase separation phenomena in aqueous solution. What uses this frustrated phase separation behavior might be put to remain an open question. It is easy to imagine using it to enhancing nanoparticle labeling with yet another conjugate. To our knowledge, however, this type of behavior has not been previously reported and could be of interest to applications involving the fine-tuning of the surface properties of the nanoparticles.

dx.doi.org/10.1021/nl201303q |*Nano Lett.* 2011, 11, 2551–2554

AUTHOR INFORMATION

Corresponding Author
*E-mail: zare@stanford.edu.

ACKNOWLEDGMENT

We thank Peng Guo for help with recording TEM images. This work was supported by the National Science Foundation under CBET-0827806.

REFERENCES

(1) Balazs, A. C.; Emrick, T.; Russell, T. P. *Science* **2006**, *314*, 1107–1110.
(2) Wang, D.; Xin, H. L.; Yu, Y.; Wang, H.; Rus, E.; Muller, D. A.; Abruna, H. D. *J. Am. Chem. Soc.* **2010**, *132*, 17664–17666.
(3) Nel, A. E.; Mädler, L.; Velegol, D.; Xia, T.; Hoek, E. M. V.; Somasundaran, P.; Klaessig, F.; Castranova, V.; Thompson, M. N. *Nat. Mater.* **2009**, *8*, 543–557.
(4) Jarvie, H. P.; King, S. M. *Nano Today* **2010**, *5*, 248–250.
(5) Gao, W. P.; Liu, W. G.; Christensen, T.; Zalutsky, M. R.; Chilkoti, A. *Proc. Natl. Acad. Sci. U.S.A.* **2010**, *107*, 16432–16437.
(6) Ge, J.; Lu, D.; Liu, Z.; Liu, Z. *Biochem. Eng. J.* **2009**, *44*, 53–59.
(7) Yan, M.; Ge, J.; Liu, Z.; Ouyang, P. *J. Am. Chem. Soc.* **2006**, *128*, 11008–11009.
(8) Ge, J.; Yan, M.; Lu, D.; Zhang, M.; Liu, Z. *Biochem. Eng. J.* **2007**, *36*, 93–99.
(9) Stayton, P. S.; Shimoboji, T.; Long, C.; Chilkoti, A.; Chen, G.; Harris, J. M.; Hoffman, A. S. *Nature* **1995**, *378*, 472–474.
(10) Jablonski, J. *Acta Phys. Pol.* **1955**, *XIV*, 295–307.
(11) Kawski, A. *Photochem. Photobiol.* **1983**, *38*, 487–508.
(12) Rubinstein, M.; Colby, R. H. *Polymer Physics*; Oxford University Press: New York, 2003.
(13) Wright, A. K.; Thompson, M. R. *Biophys. J.* **1975**, *15*, 137–141.
(14) Casalini, R.; Roland, C. M.; Capaccioli., S. *J. Chem. Phys.* **2007**, *126*, 184903.
(15) Vandenburg, H. J.; Clifford, A. A.; Bartle, K. D.; Carlson, R. E.; Carroll, J.; Newton, I. D. *Analyst* **1999**, *124*, 1707–1710.
(16) Hansen, C. M. *Hansen solubility parameters: a user's handbook*; CRC Press, Inc.: Boca Raton FL, 2007.